Application of electron backscatter diffraction to the study on orientation distribution of intermetallic compounds at heterogeneous interfaces (Sn/Ag and Sn/Cu)

H. F. Zou[1,2] and Z. F. Zhang[1,a)]
[1]*Shenyang National Laboratory for Materials Science, Institute of Metal Research, Chinese Academy of Sciences, Shenyang 110016, People's Republic of China*
[2]*Science and Technology on Reliability Physics and Application of Electronic Component Laboratory, Guangzhou 51060, Guangdong, People's Republic of China*

(Received 27 June 2010; accepted 26 September 2010; published online 23 November 2010; publisher error corrected 1 December 2010)

In the current study, the orientation distribution and formation mechanism of intermetallic compounds (IMCs) at heterogeneous interfaces (Sn/Ag or Sn/Cu) were investigated by using electron backscatter diffraction (EBSD) method. The EBSD orientation maps have revealed that some special orientation relationships exist not only at the interfaces between the faceted IMC and (001) or (111) single crystal substrates but also at the interfaces of the scalloplike IMC/(011) single crystal substrate, which are attributed to the low misfit between the IMC and the substrates. However, only part of special orientation relationships can be obtained by using the pole figure when a large number of IMC grains were considered. The reason is that the single crystal substrate can supply more immobile atoms for these special orientated IMC cluster. With increasing the reflowing or aging time, the orientation relationship has no obvious change between the IMC and the single crystal substrates. Meanwhile, it is found that the determinative factor controlling the IMC morphology should include two kinds of interfacial energies at the interfaces of IMC/solder and IMC/substrate. The variations in the interfacial energies would induce the transformation of the IMC morphology. These experimental results would be helpful for better understanding on the formation mechanisms of IMCs at the interfaces of Sn/crystals and promoting the wide application of EBSD to study the orientation relationships at other heterogeneous interfaces. © *2010 American Institute of Physics*. [doi:10.1063/1.3505796]

I. INTRODUCTION

The SnPb/Cu soldering interface is one of the typical heterogeneous interfaces which are ubiquitous in daily life. Nowadays, this soldering interface is used not only in second-level packaging, but also in first-level and zero-level packaging.[1] However, the Sn–Pb alloys would be replaced by the Pb-free alloys in the future because of the environmental and health hazard concerns regarding Pb.[2–4] In this case, abundant researches mainly concentrate on the Pb-free/Cu interfaces, including the interfacial reaction, the wetting behavior and the mechanical properties.[2,3] Among these aspects, the interfacial reactions have been paid much attention by the researchers because the essence of soldering interface achieves the electrical and mechanical interconnect by the formation of a thin intermetallic compound (IMC) layer during the interfacial reaction procedure.[2–4] These results have reported that the scalloplike Cu_6Sn_5 grains would be randomly formed on the polycrystalline Cu substrate during the reflowing procedure, which has been explained by the ripening model.[2–5]

However, recently, some new findings indicate that there are several orientation relationships between (001) and (111) Cu single crystal substrates and the Cu_6Sn_5 grains with special morphology: $[\bar{2}01]_{Cu_6Sn_5}\|[\bar{1}10]_{(001)Cu}$.[6–8] Similar orientation relationship has also been found between (001) Ag single crystal and Ag_3Sn grains: $[100]_{Ag_3Sn}\|[\bar{1}10]_{(001)Ag}$.[9] But it should be noticed that there is one $[\bar{1}10]$ direction on the (011) Cu, (011) Ag, and (111) Ag single crystal, which gives rise to an interesting question: whether similar orientation relationships ($[100]_{Ag_3Sn}\|[\bar{1}10]_{(001)Ag}$ or $[\bar{2}01]_{Cu_6Sn_5}\|[\bar{1}10]_{(001)Cu}$) can exhibit on (011) Cu, (011), and (111) Ag single crystal substrates or not. If yes, how about the texture of the IMCs formed on these single crystal substrates and how to characterize the corresponding experimental results?

In order to solve the above problems, the orientations of IMC grains and substrate should be first obtained at the same time. Obviously, it is impossible to obtain the grain orientation and the texture of IMC grains by using transmission electron microscopy (TEM) because TEM only concentrates on the small local region, including several grains.[10] However, it is well known that automated electron backscatter diffraction (EBSD) technique in scanning electron microscope (SEM) is a powerful tool for the analysis of orientation distribution of numerous grains.[11] Unfortunately, a large number of papers about the EBSD mainly concentrate on the analysis of various single-phase materials.[12–14] Only few EBSD researches were carried out on the heterogeneous in-

a)Electronic mail: zhfzhang@imr.ac.cn.

terfaces of the materials because it is very difficult to prepare for the sample compared with the single-phase materials.[10,15–17] Thus, in this study, EBSD is expected to be further applied to analyze the orientation distribution of the formed IMC grains at the heterogeneous interfaces (Sn/Ag or Sn/Cu as examples). Although electromigration induced damage strongly depends on Sn grain orientation in Pb-free solders,[17] this study did not pay much attention on the orientation of beta-Sn. Instead, we will focus on the orientation maps to reveal the formation mechanism of the IMC on the single crystal substrates.

II. EXPERIMENTAL PROCEDURE

It has been mentioned that the orientation relationship has also been detected between (001) Ag single crystal and Ag_3Sn grains.[9] Whether there are orientation relationships between other single crystals and Ag_3Sn grains or not? In order to confirm it, (011), (111), and (348) Ag single crystals were selected as substrates. Meanwhile, in order to reveal the effect of grain boundary and grain size of Cu on the formation of IMC, some Cu plates with different grain sizes were used as substrates. In our study, (011), (111) Cu single crystals, cold-drawn polycrystalline Cu with grain size of ~ 50 μm, and the ultrafined-grained Cu with grain size of ~ 2 μm made by equal-channel angular pressing (ECAP) were utilized as substrates.[18] All the substrates were ground with 800#, 1000#, 2000# SiC paper, and then carefully polished with the 2.5, 1.5 and 0.5 μm polishing pastes. Wetting samples (Sn/Cu) and sandwich samples (Cu/Sn/Cu) were prepared at 260 °C and then were cooled in air to room temperature. These couples were deeply etched with the $5\%HCl+3\%HNO_3+CH_3OH$ (wt %) etchant solution to remove the excess Sn phase so that the reactive phases can be completely exposed. But the sandwich samples were spark-cut to form some thin plates (about 500 μm thick) with dimensions of $10\times10\times0.6$ mm^3. In order to prepare the EBSD samples, these thin sandwiches were then mechanically ground to a final thickness of about 100 μm, and then carefully polished with the 2.5, and 1.0 μm polishing pastes, finally ion-milled at 5.0 KeV and 4–6 μA with a low milling angle (10°–12°) for ~ 1 h. The morphology of the IMCs was observed by the LEO Supra 35 field SEM. Orientation maps were then collected on the selected area using a SEM equipped with a fully automatic EBSD analysis system (Oxford Instruments-HKL Channel). During the EBSD acquisition, a step size of 0.3–0.6 μm was chosen.

III. EXPERIMENTAL RESULTS

A. IMC morphologies formed on Cu and Ag single crystals with different orientations

Figure 1(a) is the top-view SEM image of Ag_3Sn grains formed on (001) Ag single crystal reflowed at 260 °C. It can be seen that there are many regular faceted-Ag_3Sn grains with parallel edges formed on (001) Ag single crystal, which has been reported in our previous paper[9] but it is inconsistent with the Choi's description.[19] The elongations of Ag_3Sn grains formed on (001) Ag single crystal are similar to the Cu_6Sn_5 grains formed on (001) Cu single crystal.[8] When the orientation of Ag substrate changes into (011), the morphology of the formed Ag_3Sn grains is still faceted, but irregular faceted, which was not observed on (011) Cu single crystal,[8] as illustrated in Fig. 1(b). The irregular faceted Ag_3Sn grains were also detected on (111) and (348) Ag single crystals, as displayed in Figs. 1(c) and 1(d). It is indicated that the regular faceted Ag_3Sn grains only formed on (001) Ag single crystal while the irregular faceted Ag_3Sn grains can form on other Ag single crystals [such as (011), (111), etc.], which is different from that on Cu single crystal.[8]

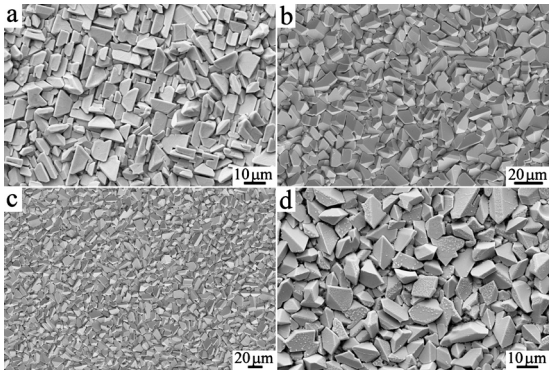

FIG. 1. Morphology of Ag_3Sn grains formed on different orientated Ag single crystals (a) (001); (b) (011); (c) (111); and (d) (348).

The typical scalloplike Cu_6Sn_5 grains were observed on the coarse-grained, ultrafine-grained Cu and (011) Cu single crystal, which is completely different from that on (111) Cu single crystal, as displayed in Fig. 2. It has been reported that there are several orientation relationships between the prism-type IMC and Cu substrate.[8] Are there any special orientation relationships between the irregular IMC grains and substrate? In order to investigate it, the EBSD method was used in this study and numerous IMC grains were tested to reveal the texture of IMC. All detailed results will be given as below.

B. Phase and orientation maps across the cross-section of Sn/Cu and Sn/Ag couples

Figure 3(a) shows the cross-section phase maps of Sn/(111)Ag couple aged at 170 °C for 10 days. The red, blue, green regions represent Sn, Ag_3Sn and Ag phase in Fig. 3(a),

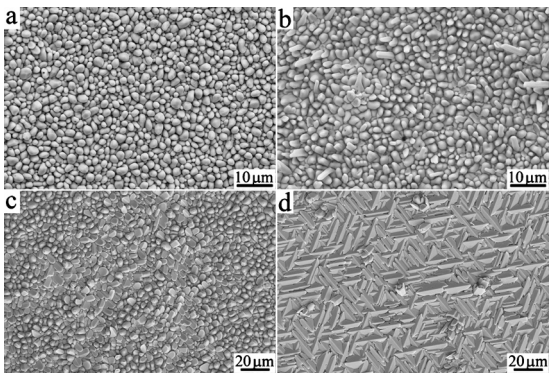

FIG. 2. Morphology of Cu_6Sn_5 grains formed on (a) ECAPed Cu; (b) cold-drawn Cu; (c) (011) Cu single crystal; and (d) (111) Cu single crystal.

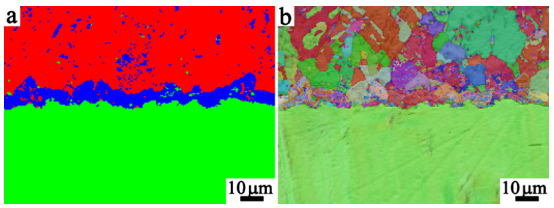

FIG. 3. (Color online) EBSD maps for the Sn/(111) Ag couples: (a) phase map and (b) orientation map.

respectively; obviously, a lot of Ag_3Sn grains were detected in the solder. The corresponding orientation maps are shown in Fig. 3(b).

In order to further investigate the effect of grain size on the formation of the IMC, three kinds of Cu substrates were employed: i.e., ECAPed, cold-drawn, and (011) Cu single crystal. Figure 4(a) presents the cross-section phase maps of the ECAPed Cu/Sn. The blue, green, red regions represent Sn, Cu_6Sn_5, and ECAPed Cu, respectively. At the ECAPed Cu/Sn interface, few Cu_6Sn_5 grains were detected in the Sn phase with many striplike Sn grains compared with the Ag/Sn couple because the solubility of Cu in the liquid Sn is lower than that of Ag.[3,20] The optimal growth direction of Cu_6Sn_5 grains is along the grain boundaries of Sn phase and individual Cu_6Sn_5 grain can cover several Cu grains, indicating that the grain boundary did not impede the coarsening of Cu_6Sn_5 grains, as displayed in Fig. 4(b). Similar to the ECAPed Cu/Sn interface, the cold-drawn Cu/Sn interface is still rather rough, as displayed in Figs. 4(a) and 4(c). Some abnormal Cu_6Sn_5 grains with large height-width ratio seriously embedded into the Sn phase along the grain boundaries, as illustrated in Fig. 4(d). In contrast, the Cu_6Sn_5 grains with small height-width ratio formed on (011) Cu single crystal substrate, as displayed in Fig. 4(e).

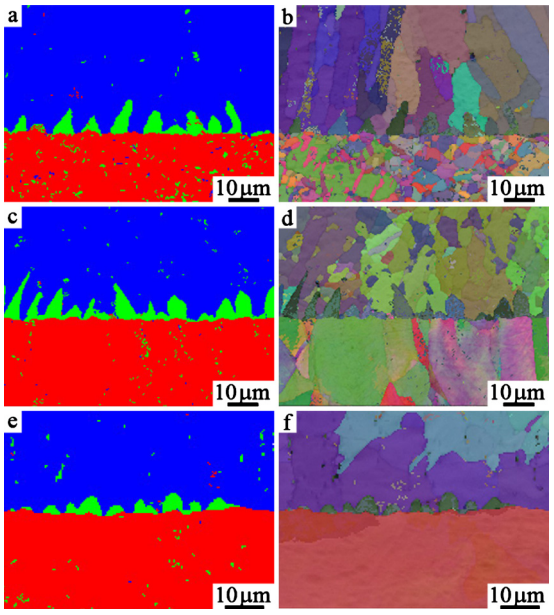

FIG. 4. (Color online) EBSD maps: (a) and (b) phase and orientation maps for ECAPed Cu/Sn couple; (c) and (d) phase and orientation maps for cold-drawn Cu/Sn couple; and (e) and (f) phase and orientation maps for Sn/(011) Cu single crystal couple.

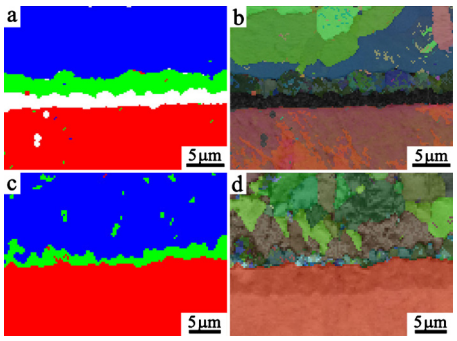

FIG. 5. (Color online) EBSD phase and orientation maps for the Sn/(011) Cu single crystal couples aged at: (a) and (b) 170 °C for ten days and (c) and (d) 50 °C for ten days.

In addition, the grain size of Sn phase is rather large for the Cu single crystal substrate compared with the ECAPed and cold-drawn Cu substrates, furthermore, the Sn phase mainly concentrates on the two orientations in the selected region, as displayed in Fig. 4(e). As a result, it can be concluded that the grain size of Cu substrate can affect the morphology of Cu_6Sn_5 and the grain size of Sn phase.

On the other hand, it is well known that the new phase (Cu_3Sn) will always appear at the Cu/Cu_6Sn_5 interface for the Cu/Sn couples aged at high temperature for long time. As a result, the complete orientation map is not able to be obtained for the cross-section of Cu/Sn couple aged at 170 °C for 10 days because the orientation of Cu_3Sn superlattice structure cannot be indexed by using EBSD, as demonstrated in Figs. 5(a) and 5(b). But only one thin Cu_6Sn_5 layer was observed at the interface for the Cu/Sn couple aged at 50 °C for 10 days, which is similar to the other reports,[1] as displayed in Fig. 5(c). Based on the orientation map in Fig. 5(d), all the Cu_6Sn_5 grains display the similar color, indicating that they have the approximately same orientation.

C. Texture formation of the IMC on single crystal substrates

1. Effect of crystal orientation on the texture formation of IMC

In order to obtain the texture of IMC, a lot of grains at the Ag/Sn or Sn/Cu interfaces were analyzed by using EBSD. These orientation maps would first be merged together to highlight the projects with the help of the software of CHANNEL 5. Then the orientation data of Ag_3Sn grains, Ag single crystal were separated by using the CHANNEL 5. Finally, the inverse pole figure (IPF) and the pole figure (PF) would be easily gotten.

Figures 6(a)–6(c) exhibits the IPF and PF of the Sn/(011) Ag single crystal couple reflowed at 260 °C for 10 min. Corresponding to the Ag_3Sn phase, the rolling direction (RD) shows weak $\sim[\bar{2}16]$ texture, as shown in Fig. 6(a). According to Figs. 6(b) and 6(c), one orientation relationship can be gotten: $\{110\}_{Ag}\|\{010\}_{Ag_3Sn}$, which is consistent with that at the Sn/(001) Ag couple.[9] In order to further investigate the orientation effect of Ag single crystal, (111) and (348) Ag single crystals were also selected as substrates to react with molten Sn. Based on their RD IPFs, the statistical

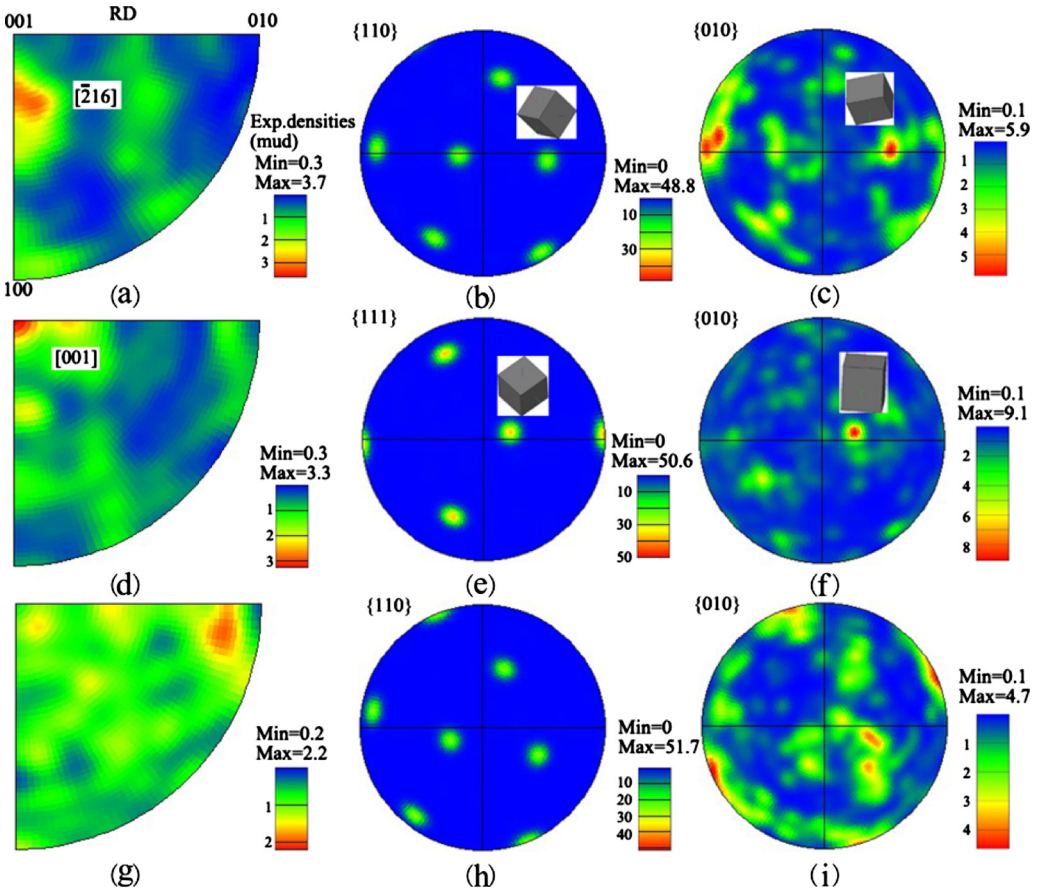

FIG. 6. (Color online) PFs and IPFs of the couple reflowing at 260 °C for 10 min: (a) the IPF of Ag_3Sn, (b) the PF of Ag, (c) the PF of Ag_3Sn for the Sn/(011) Ag couple; (d) the IPF of Ag_3Sn, (e) the PF of Ag, (f) the PF of Ag_3Sn for the Sn/(111) Ag couple; (g) the IPF of Ag_3Sn, (h) the PF of Ag, and (i) the PF of Ag_3Sn for the randomly orientated Ag/Sn couple.

results confirm that the Ag_3Sn grains also exhibit strong [001] texture on (111) Ag single crystal substrate, as demonstrated in Fig. 6(d). According to the PFs, the orientation relationship can be also obtained: $\{111\}_{Ag}\|\{010\}_{Ag_3Sn}$, as displayed in Figs. 6(e) and 6(f).

Figures 6(g)–6(i) show the IPFs and PFs of the Ag_3Sn grains for the couple between Sn and (348) Ag single crystal. The orientations in RD IPF of the Ag_3Sn grains become rather dispersive compared with on (011) and (111) Ag single crystal substrates, as illustrated in Figs. 6(a), 6(d), and 6(g). Based on the PFs in Figs. 6(h) and 6(i), there is no a special orientation relationship between Ag and Ag_3Sn grains. Combining with the above experimental results, it can be concluded that the orientation of Ag substrate determines the crystallographic relationship between Ag and Ag_3Sn grains.

2. Effect of reflowing or aging time on the texture formation of IMC

The orientation effect of Ag single crystal on the texture formation of IMC has been discussed in Sec. III C 1. In this section, the effect of aging or reflowing time on the texture of IMC will be further analyzed. Figures 7(a)–7(f) show the texture of the Sn/(110) Ag single crystal joint reflowed at 260 °C for different times. For the Ag_3Sn grains, with increasing the reflowing time, the RD IPF has no obvious change, as displayed in Figs. 6(a), 7(a), and 7(d). Based on the PFs of Ag and Ag_3Sn grains in Figs. 7(b) and 7(c), the following orientation relationships can also be obtained: $\{110\}_{Ag}\|\{010\}_{Ag_3Sn}$ and $\{111\}_{Ag}\|\{100\}_{Ag_3Sn}$. However, other orientation relationship was not detected when the reflowing time is only 10 min, as displayed in Figs. 6(b) and 6(c). When the reflowing time further increases to 30 min, the RD IPF of Ag_3Sn phase is similar to that reflowing for 20 min, forming a strong [$\bar{1}$04] texture, as illustrated in Figs. 7(a) and 7(d). And only one orientation relationship was obtained: $\{110\}_{Ag}\|\{010\}_{Ag_3Sn}$, as illustrated in Figs. 7(e) and 7(f). Combining with Figs. 6 and 7, it can be concluded that the reflowing time does not affect the texture and the orientation relationship between Ag and Ag_3Sn grains.

Figures 7(g)–7(i) show the orientation maps of the Sn/(110) Ag single crystal couple aged at 170 °C for ten days. It is surprising to see that the orientation relationship has no change compared with the as-reflowed couple. But the pole density maximum of RD IPF has slight decrease compared with that under the liquid-state aging condition, as illustrated in Fig. 6(a) and 7. It is indicated that the Ag_3Sn nucleus, which formed at the reflowing initial stage, would gradually grow with increasing aging time.

In addition, the Sn/(111) Ag single crystal couple reflowed for 30 min was also investigated. From the IPFs and PFs of Ag_3Sn phase, a strong (001) texture still emerges along the RD, and the orientation relationship has no obvious

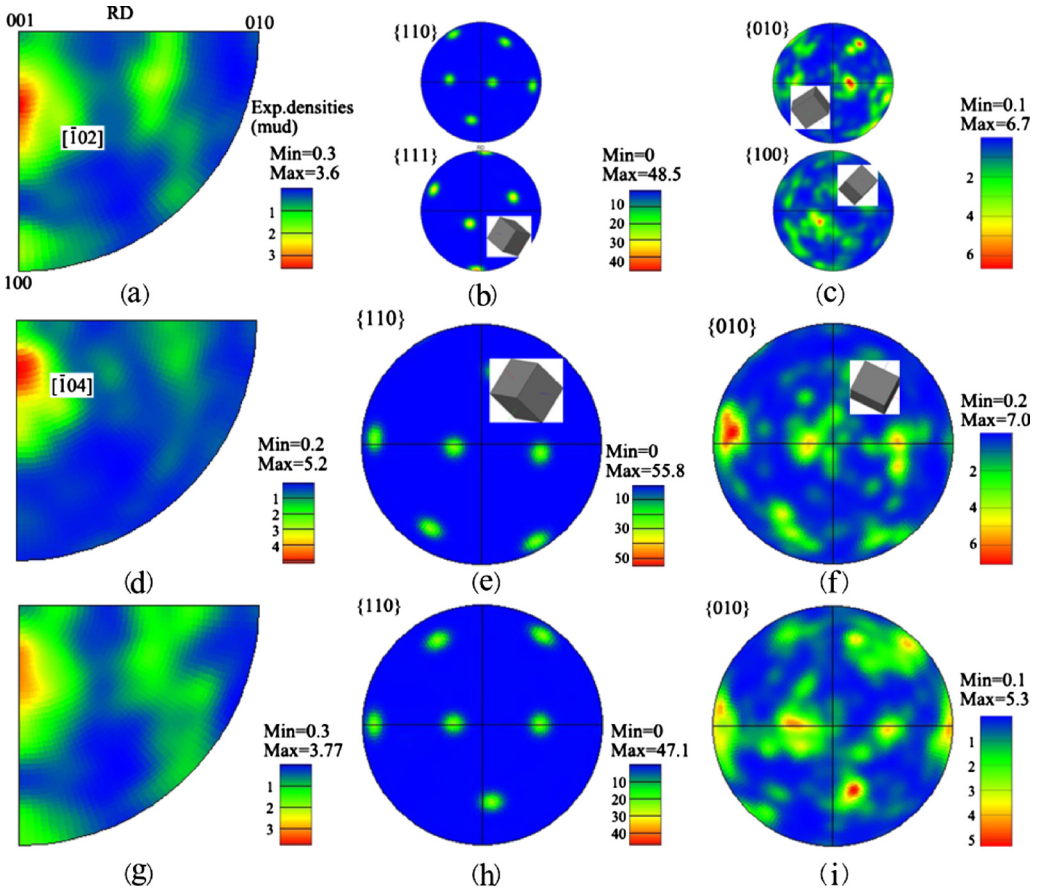

FIG. 7. (Color online) PFs and IPFs of the Sn/(011)Ag couple: (a) the IPF of Ag_3Sn, (b) the PF of Ag, (c) the PF of Ag_3Sn for the couple reflowing at 260 °C for 20 min; (d) the IPF of Ag_3Sn, (e) the PF of Ag, (f) the PF of Ag_3Sn for the couple reflowing at 260 °C for 30 min; (g) the IPF of Ag_3Sn, (h) the PF of Ag, and (i) the PF of Ag_3Sn for the couple reflowing at 170 °C for ten days.

change with increasing the reflow time compared with the6couples reflowed for 10 min, as presented in Figs. 6(g)–6(i) and Figs. 8(a)–8(c). The results further confirm that the IMC formed at the reflowing initial stage plays a decisive role in the development of the orientation relationship between the substrate and the IMC grains.

3. Effect of grain size on the texture formation of IMC

The IPFs and PFs of Cu_6Sn_5 grains formed on (011) Cu single crystal were obtained and displayed in Fig. 9. The texture intensity of Cu_6Sn_5 grains is extremely stronger than that of Ag_3Sn grains formed on Ag single crystal

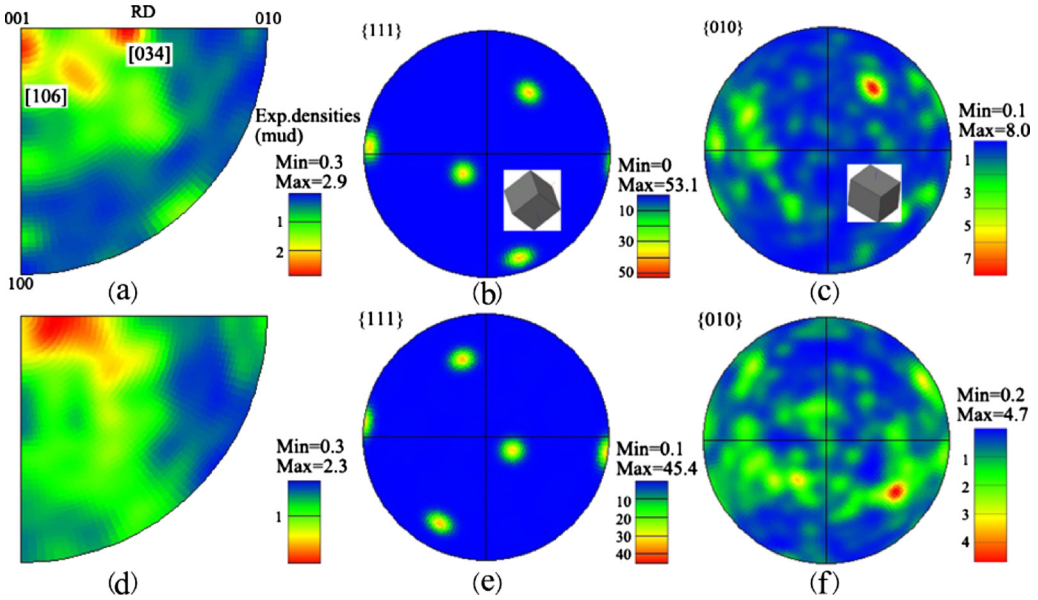

FIG. 8. (Color online) PFs and IPFs of the Sn/(111)Ag couple: (a) the IPF of Ag_3Sn, (b) the PF of Ag, (c) the PF of Ag_3Sn for the couple reflowing at 260 °C for 30 min; (d) the IPF of Ag_3Sn, (e) the PF of Ag, and (f) the PF of Ag_3Sn for the coupled reflowing at 170 °C for ten days.

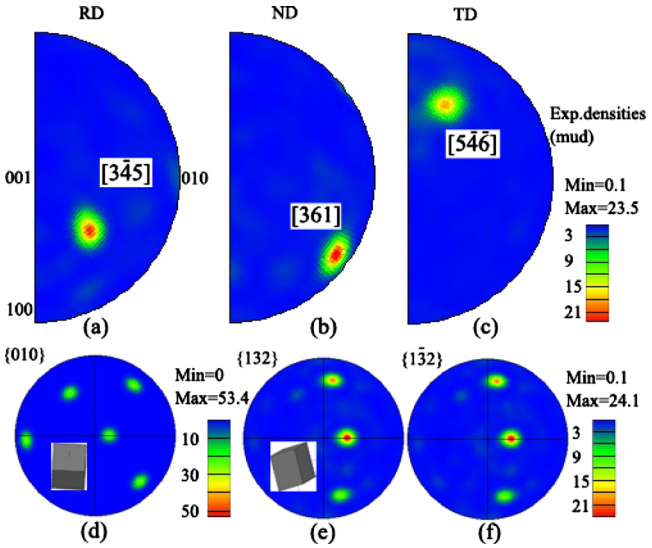

FIG. 9. (Color online) [(a)–(c)] IPFs of Cu_6Sn_5; (d) the PF of Cu (e) and (f) the PFs of Cu_6Sn_5 for the as-reflowed Sn/(011)Cu couple.

(maximum=23.5 for Cu_6Sn_5, and 3.7 for Ag_3Sn), as displayed in Fig. 6 and 9(a)–9(c). According to these PFs in Figs. 9(e) and 9(f), the orientation relationships between Cu_6Sn_5 grains and (011) Cu single crystal can be identified as: $\{110\}_{Cu}\|\{132\}_{Cu_6Sn_5}$, $\{110\}_{Cu}\|\{1\bar{3}2\}_{Cu_6Sn_5}$, which are the same as that at the individual cross-section of Cu/Sn.[10] When the ECAPed and cold-drawn Cu were used as substrate, such orientation relationships cannot be found from the PFs (thus, we did not list the PFs). The IPFs are indicated that the texture along TD is much weaker compared with that on the Cu single crystal substrate, as displayed in Fig. 9 and Fig. 10(b). From the TD IPFs, it can be concluded that the Cu substrate shows weak [111] texture, but the position of the pole density maximum of Cu_6Sn_5 is different, as demonstrated in Fig. 10. Therefore, the grain size of the Cu substrate can slightly affect the texture of the IMC layer.

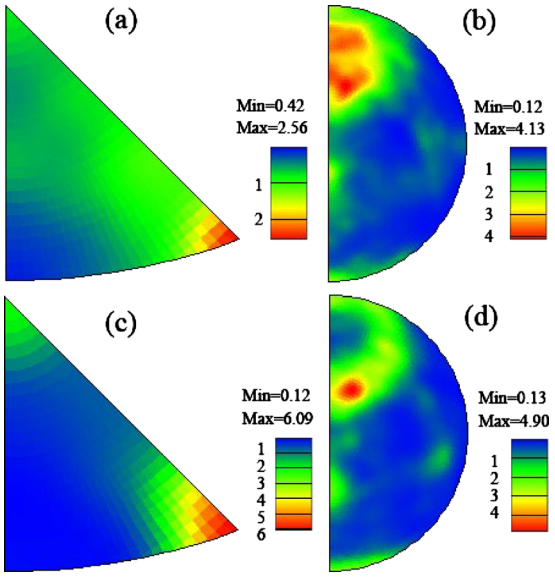

FIG. 10. (Color online) Inverse PFs (a) Cu; (b) Cu_6Sn_5 for the as-reflowed Sn/ECAPed Cu couple; (c) Cu; and (d) Cu_6Sn_5 for the as-reflowed Sn/cold-drawn Cu couple.

Figure 11 shows the PFs of the Sn/(110) Cu couple aged at 50 °C for 10 days. Based on the phase maps, it can be easily found that only Cu_6Sn_5 IMC layer formed at the Cu/Sn interface, as displayed in Figs. 4(e) and 4(f). From these PFs, some orientation relationships can be obtained as below

$$\{110\}_{Cu}\|\{132\}_{Cu_6Sn_5}, \quad \{110\}_{Cu}\|\{1\bar{3}2\}_{Cu_6Sn_5},$$

$$\{110\}_{Cu}\|\{102\}_{Cu_6Sn_5},$$

$$\{111\}_{Cu}\|\{010\}_{Cu_6Sn_5}, \quad \{111\}_{Cu}\|\{112\}_{Cu_6Sn_5},$$

$$\{111\}_{Cu}\|\{1\bar{1}2\}_{Cu_6Sn_5}.$$

Compared with the as-reflowed couples, some new orientation relationships can be observed, as displayed in Figs. 9 and 11. In addition, the H-type Cu_6Sn_5, which was encircled by seven Sn grains, was further investigated, as displayed in Fig. 12. According to these poles of Sn grains and the Cu_6Sn_5 grains, it is surprising to find that there is an orientation relationship ($\{02\bar{2}\}_{Sn}\|\{71\bar{2}\}_{Cu_6Sn_5}$) between Cu_6Sn_5 and Sn phase, which is the same as Shang's result,[21] as illustrated by the PFs in Figs. 12(a)–12(c). Whether the orientation of Cu_6Sn_5 grains can also affect the orientation of beta-Sn or not, it would need much work to determine in the future because the orientation of beta-Sn can determine the lifetime of solder joint.[17]

However, the Cu_3Sn layer would form at the Cu_6Sn_5/Cu interface when the aging temperature is above 60 °C.[1] It has also been reported that the formation of Cu_3Sn layer would induce the morphology transformation of the Cu_6Sn_5 grains from prismlike to scalloplike.[8] In this case, does the change in the morphology of Cu_6Sn_5 grains induce some change about the texture of Cu_6Sn_5 grains? Figure 13 shows the IPFs and PFs of the Cu_6Sn_5 phase when the Sn/Cu couples were aged at 170 °C for 10 days. The phase maps in Fig. 5(a) have confirmed that the Cu_3Sn layer formed at the Cu_6Sn_5/Cu interface. However, the IPFs texture intensity of the Cu_6Sn_5 grains has no evident variety compared with that of the as-reflowed couple, as illustrated in Figs. 9(c) and 9(d) and Figs. 13(c) and 13(d). The position of the pole density maximum has changed compared with the as-reflowed couple, which should be attributed to the change in the Cu substrate because the orientation of Cu substrate might have a small change during the grinding procedure. The experimental results imply that the formation of the Cu_3Sn grains should not affect the IPFs texture intensity of Cu_6Sn_5 grains during the following aging procedure.

IV. DISCUSSION

A. Orientation relationship of IMC/substrate and IMC/solder

As mentioned above, some preferential orientation relationships might exist between the Ag_3Sn phase and (011) Ag single crystal. To further investigate the orientation relationship between the Ag_3Sn and (011) Ag single crystal, individual orientation map was selected to carefully analyze. Figure 14(a) shows the 3D unit cells model of the Ag sub-

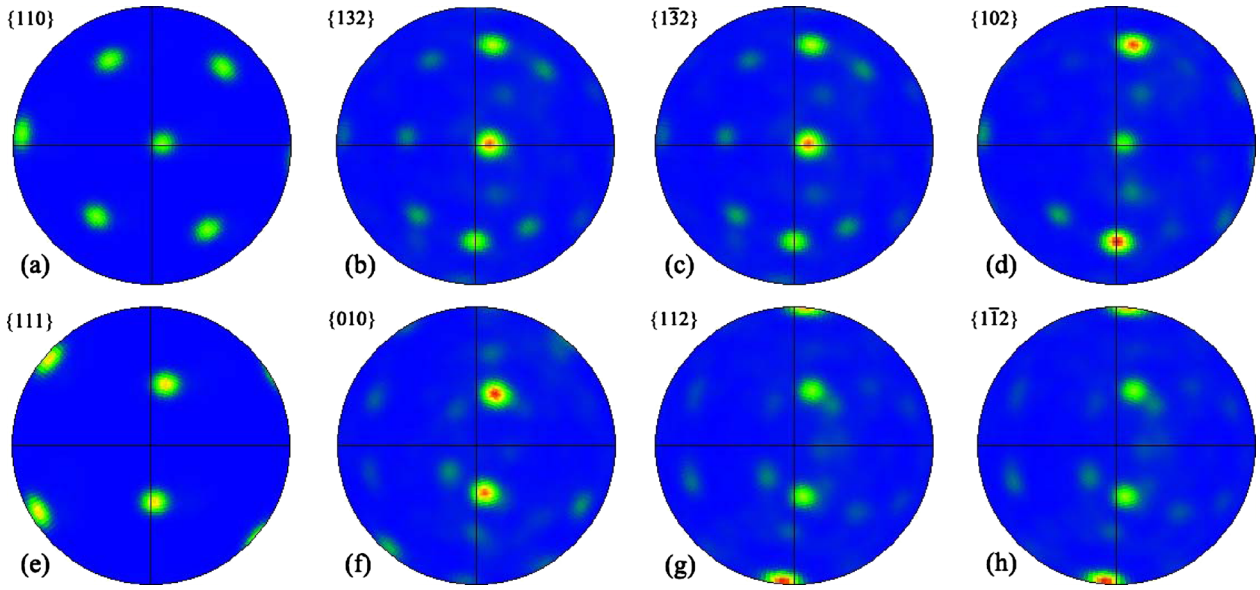

FIG. 11. (Color online) PFs of (a) and (e) Cu; [(b)–(d)] and [(f)–(h)] Cu_6Sn_5 for Sn/(011)Cu reflowed at 50 °C for ten days.

strate and Ag_3Sn grains formed on the Ag substrate. Figure 14(b) visually describes the separation of the Ag substrate and Ag_3Sn grains. Figures 14(c)–14(g) show the PFs of (011) Ag, the PFs of Ag_3Sn unit cell in Fig. 14(a). Based on these PFs, four kinds of orientation relationships between the Ag_3Sn grains and (011) Ag single crystal can be obtained as below

$$\{1,1,0\}_{Ag} \| \{0,16,25\}_{Ag_3Sn}, \quad \{1,1,0\}_{Ag} \| \{0,1,0\}_{Ag_3Sn},$$

$$\{1,1,0\}_{Ag} \| \{0,8,25\}_{Ag_3Sn}, \quad \{1,1,0\}_{Ag} \| \{0,0,1\}_{Ag_3Sn}.$$

The experimental results above provide clear evidences that the orientation relationships not only exist between the regular faceted Ag_3Sn grains and (001) Ag single crystal but also between the irregular faceted Ag_3Sn grains and (011) Ag single crystal. The atom misfit would be considered to explain this phenomenon. Figure 15(a) demonstrates the arrays of Ag atoms of (110) plane in Ag single crystal along $[\bar{1}10]$ direction. It is known that the Ag atom space is 0.2889 nm along [110] direction. Figure 15(b) presents the arrays of Ag atoms in Ag_3Sn along [100] direction. Based on the structure of Ag_3Sn phase (*Pmmm*, $a=0.5969$ nm, $b=0.4780$ nm, and $c=0.5184$ nm),[22] it can be easily obtained that the distance of two continuous Ag atoms is 0.2984 nm along [100] direction. In this case, the misfit of Ag atoms (β_{Ag}) between the [100] direction of Ag_3Sn and the [110] direction of Ag single crystal can be gotten

$$\beta_{Ag} = (0.2984 - 0.2889)/0.2984 = 3.18\%. \quad (1)$$

According to this result, it can be easily found that the misfit of Ag atoms is very small at these two heterogeneous planes. As a result, in order to minimize the interfacial energy, the Ag_3Sn grains would preferentially nucleate along [110] direction on (011) Ag single crystal. Considering the cell structure of Ag_3Sn grain in Fig. 15(b), four planes, i.e., (010), (001), (0 8 25), and (0 16 25) should involve along [100] direction.

Since the Ag atom space is 0.2889 nm along [110] direction on (111) plane, there should be also special orientation relationship between (111) Ag single crystal and Ag_3Sn

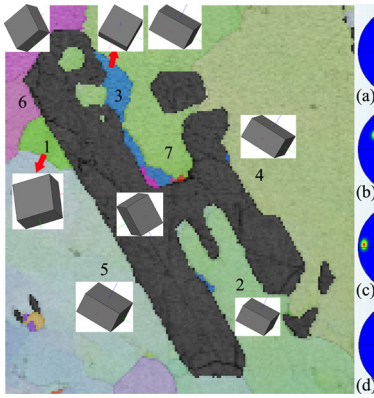

FIG. 12. (Color online) (a) $\{71\bar{2}\}$ PF of Cu_6Sn_5, [(b)–(h)] $\{02\bar{2}\}$ PFs of Sn.

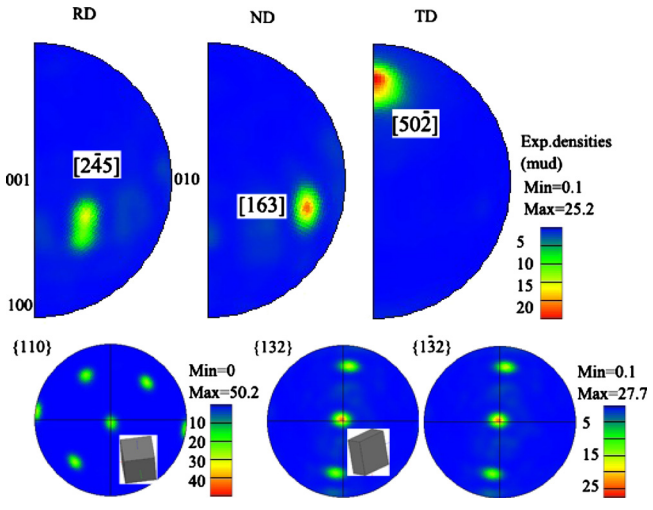

FIG. 13. (Color online) [(a)–(c)] IPF of Cu_6Sn_5; (d) PF of Cu (e) and (f) PFs of Cu_6Sn_5 for Sn/(011)Cu reflowed at 170 °C for 10 days.

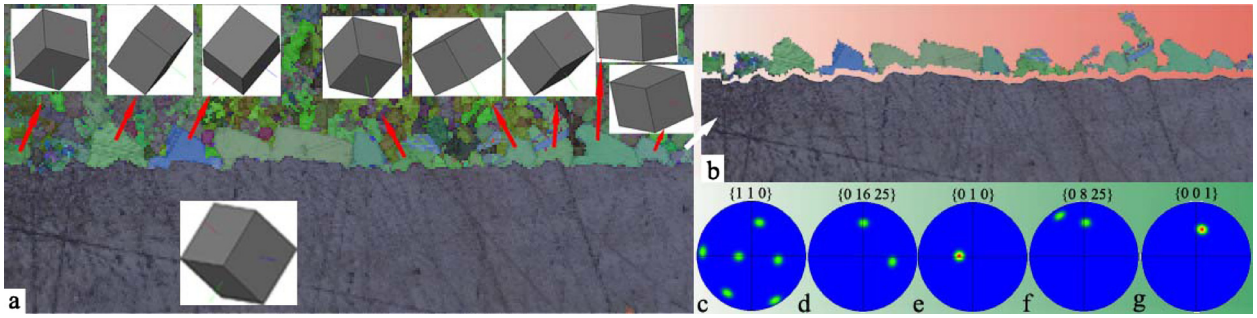

FIG. 14. (Color online) EBSD maps (a) and (b) phase map of Sn/(011) Ag; PF (c) Ag single crystal, [(d)–(g)] Ag_3Sn grains.

phase, as displayed in Figs. 6(h) and 6(i). But regular faceted IMCs were not formed on (111) Ag single crystal, which is not consistent with that on (111) Cu single crystal.[8] And the texture intensity of Cu_6Sn_5 grains is extremely stronger than that of Ag_3Sn grains formed on Ag single crystal, as displayed in Fig. 6 and Figs. 9(a)–9(c). It should be attributed to the different misfit. For Cu/Sn couple, the misfit of Cu atoms between Cu and Cu_6Sn_5 is only 0.32%, which is much lower than that (3.18%) of Ag atoms between Ag and Ag_3Sn.[8,9] Combining with the previous experimental results,[8–10] the morphologies of IMC and all the orientation relationships (including Ag and Cu) are summarized in Table I. In summary, it is the misfit between the IMC and single crystal substrate that is very important for the texture formation and the morphology of IMC.

B. Formation mechanism of the optimal texture of IMC on Ag single crystal

The above experimental results reveal that four orientation relationships can be detected between Ag_3Sn and Ag single crystals based on the cross-sectional Ag/Sn couple, as demonstrated in Fig. 14. But only one ($\{110\}_{Ag}\|\{010\}_{Ag_3Sn}$, $\{111\}_{Ag}\|\{010\}_{Ag_3Sn}$) of orientation relationships was obtained based on the texture analysis, as displayed in Figs. 6–8. The appearance of this phenomenon should be related to the stable nucleation mechanism during reflowing procedure. It is known that the nucleation rate is[23]

$$I = I_0 \exp\left(-\frac{Q}{kT}\right). \tag{2}$$

Here, I_0 is the total number of atoms per unit, I is the number of critical nuclei per unit, Q is the activation energy to form the critical IMC grain, k_B is the Boltzmann constant, and T is the reaction temperature. According to the nucleation of the vapor deposits, Q can be written[23]

$$Q = nQ_{ad} + Q_{ad} + E_n - Q_D. \tag{3}$$

Where n is the number of atoms of the cluster, E_n is the binding energy of the cluster which is related to the size n and the structure of the cluster, Q_D is the activation energy for surface diffusion, and Q_{ad} is the additional energy of atom to form a three-dimensional nucleus. When the substrate can supply more immobile atoms for the stable cluster, the formation of the stable cluster would acquire fewer atoms from the surrounding, which decreases the total additional energy of atom to form a three-dimensional nucleus, leading to the increase in the nucleation rate.

Based on the illustrations in Figs. 15 and 16(a), the minimal immobile atoms for the stable Ag_3Sn cluster, which is supplied by the Ag single crystal substrate, contain two atoms. But it cannot determine the orientation of the Ag_3Sn cluster; therefore, it is necessary for the decision of the final orientation of the stable Ag_3Sn cluster to require the third atom, as displayed in Figs. 16(b) and 16(c). In this case, several orientation relationships would form between the Ag_3Sn grain and the Ag single crystal substrate because of the random of the third atoms, as confirmed in Fig. 15(b).

However, if more immobile atoms (three, four even more) can be directly supplied to form the special Ag_3Sn cluster, which would be easy to grow, leading to the strong texture formation of the Ag_3Sn grains. Figures 16(d)–16(f) show the Ag atoms array of (111), (110) Ag single crystals, and (010) Ag_3Sn, respectively. Obviously, there is another low misfit of Ag atoms on (111) Ag single crystal, as illus-

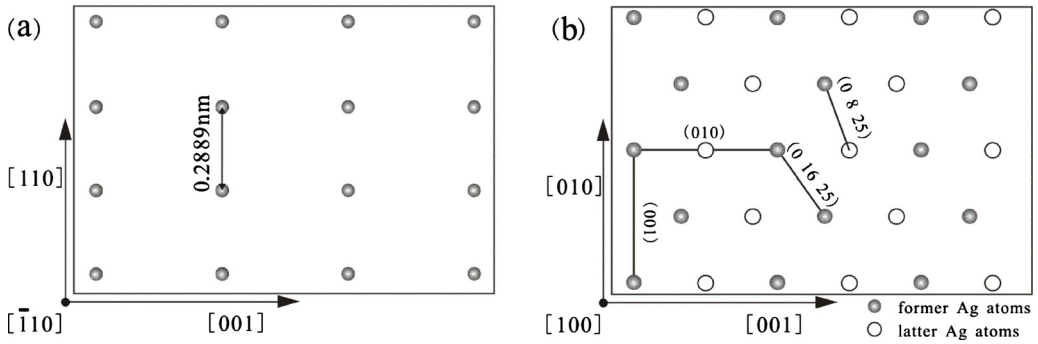

FIG. 15. (Color online) Arrays of Ag atoms (a) (110) Ag along [$\bar{1}$10] direction; (b) (100) Ag_3Sn along [100] direction.

TABLE I. Summary about the orientation relationships between Cu_6Sn_5/Cu or Ag_3Sn/Cu interfaces measured by EBSD method.

Substrate orientation	(100)	(110)	(111)	Random
Cu_6Sn_5		Scalloplike		Scalloplike
		$\{110\}_{Cu}\|\|(132)_{Cu_6Sn_5}$	Prism-type	
	Prism-type	$\{110\}_{Cu}\|\|(1\bar{3}2)_{Cu_6Sn_5}$	$\{111\}_{Cu}\|\|\{010\}_{Cu_6Sn_5}$	
	$\{100\}_{Cu}\|\|\{010\}_{Cu_6Sn_5}$	$\{110\}_{Cu}\|\|(112)_{Cu_6Sn_5}$	$\{111\}_{Cu}\|\|\{1\bar{1}2\}_{Cu_6Sn_5}$	
	$\{100\}_{Cu}\|\|\{102\}_{Cu_6Sn_5}$	$\{110\}_{Cu}\|\|(\bar{2}01)_{Cu_6Sn_5}$	$\{111\}_{Cu}\|\|\{112\}_{Cu_6Sn_5}$	
		$\{110\}_{Cu}\|\|(102)_{Cu_6Sn_5}$	$\{111\}_{Cu}\|\|\{102\}_{Cu_6Sn_5}$	
Ag_3Sn		Faceted		Faceted
	Faceted	$\{1,1,0\}_{Ag}\|\|\{0,16,25\}_{Ag_3Sn}$	Faceted	
	$(001)_{Ag_3Sn}\|\|(001)_{Ag}$	$\{1,1,0\}_{Ag}\|\|\{0,8,25\}_{Ag_3Sn}$	$\{111\}_{Ag}\|\|\{100\}_{Ag_3Sn}$	
		$\{110\}_{Ag}\|\|\{010\}_{Ag_3Sn}$	$\{111\}_{Ag}\|\|\{010\}_{Ag_3Sn}$	
		$\{110\}_{Ag}\|\|\{001\}_{Ag_3Sn}$		

trated by the broken lines in Figs. 16(d) and 16(f). And also the angle between two directions with low misfit is ~60°. It is indicated that the (111) Ag single crystal substrate is much easy to supply a (010) Ag_3Sn stable cluster compared with the other oriented Ag_3Sn grain. As a result, only one ($\{111\}_{Ag}\|\{010\}_{Ag_3Sn}$) orientation relationship can be detected by the PFs although other orientation relationships can be also obtained with the low misfit theory, as observed in Figs. 6, 8, and 14. Based on the similar analysis, (110) Ag single crystal substrate is more easy to supply a stable cluster for forming the (010) Ag_3Sn grain compared with the Ag_3Sn grain with other orientations, as displayed in Fig. 15(b).

C. Morphologies of IMCs formed on Cu and Ag substrates

As mentioned above, the prismlike Cu_6Sn_5 grains only formed on some special orientated Cu single crystals [e.g., (001) or (111)],[8] while the scalloplike Cu_6Sn_5 grains would be observed on other Cu single crystals or polycrystalline Cu.[1,8] The studies by Choi *et al.*[19] proposed that the IMC morphology is strongly dependent on the Jackson's parameter (α), which is only suitable for the pure metal.[24]

Based on the analysis of the Jackson s parameter in Choi s paper,[19] the morphologies of Cu_6Sn_5 and Ag_3Sn grains should be scalloplike. But our experimental results[8,9] provided intuitionistic evidences to confirm that the morphologies of Cu_6Sn_5 and Ag_3Sn grains can display faceted during the reflowing stage. Furthermore, it has been reported that the morphology of Cu_6Sn_5 grains would have a transformation from prismlike to scalloplike with increasing the reflow time,[8] which is not consistent with the Jackson's parameter. In addition, the Jackson's parameter was only determined by the enthalpy change during the interfacial reaction of the solder/substrate in Choi's paper,[19] obviously, there is no change about the enthalpy for the same couple under the same reactive temperature. Thus, the Jackson's parameter cannot well explain the formation mechanisms of the IMC morphology because the interfacial reaction would occur for the soldering procedure.

Here, two important factors may be considered to explore the morphology above: (1) the interfacial energy of the solder/IMC and (2) the decrease in the interfacial energy due to the orientation relationship between the IMC and substrate. Compared with the faceted Cu_6Sn_5 grains, the faceted Ag_3Sn grains would be easily formed on the Ag single crystal, as displayed in Figs. 1 and 2, which is related to the strong anisotropy of the IMC/Sn interfacial energy and the difference in the IMC/Sn interfacial energy for the different

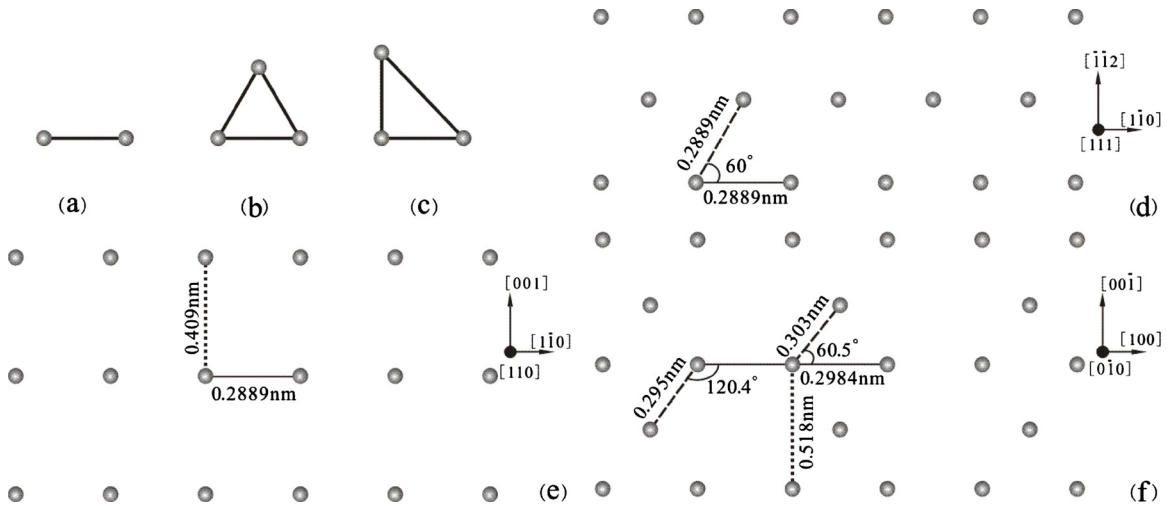

FIG. 16. (Color online) [(a)–(c)] Structure of cluster; [(d)–(f)] Ag atoms array of (111), (110) Ag single crystal, and (010) Ag_3Sn.

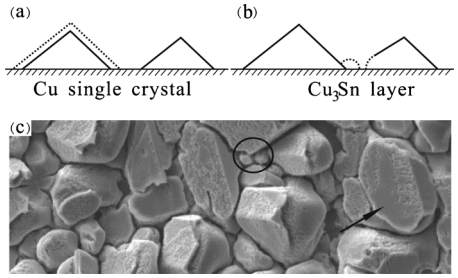

FIG. 17. Schematic illustration and morphology of Cu_6Sn_5 grains (a) without Cu_3Sn and (b) with Cu_3Sn; (c) morphology of Cu_6Sn_5 formed at Sn/(001)Cu reflowing at 260 °C for long time.

IMCs.[25] About the morphology transformation of Cu_6Sn_5 grains, the formation of the new phase (Cu_3Sn) should be considered. During the initial reflowing stage, only Cu_6Sn_5 grains were formed on the special Cu single crystals, as displayed in Fig. 17(a). Due to the extremely low misfit between the Cu single crystal and Cu_6Sn_5 grains, it would intensely decrease the interfacial energy. Then the Cu_6Sn_5 grains would be controlled to grow as the configuration of a Cu_6Sn_5 monoclinic unit cell,[6,8] as displayed in Fig. 17(a). Finally, the morphology of Cu_6Sn_5 grains shows regular facets. But with increasing the reflowing time, the appearance of the Cu_3Sn layer would destroy the low misfit interface,[8] then the Cu_6Sn_5/Cu interface has transformed into Cu_3Sn/Cu interface, leading to the rapid increase in the surface energy of Cu_6Sn_5 grain. In this case, the contact angle of Cu_3Sn/Cu_6Sn_5 would have some changes and some new scalloplike Cu_6Sn_5 nucleus would appear at the Cu_3Sn/solder interface,[8] as displayed by the broken arc in Fig. 17(b). It has been demonstrated by the experimental results, as displayed by the arrow and circle in Fig. 17(c). In this case, the new scalloplike Cu_6Sn_5 grains would gradually swallow the faceted Cu_6Sn_5 grains, indicating that the morphology of Cu_6Sn_5 grains transforms from the faceted into scalloplike with increasing reflowing time.

V. CONCLUSIONS

EBSD was successfully applied to explore the orientation relationships at the heterogeneous interfaces of Sn/Cu and Sn/Ag joints. The main conclusions can be obtained as below.

(1) The EBSD orientation maps have confirmed that the orientation relationships not only exist at the interface of the faceted IMC and some special single crystal substrates [(001), (111)] but also appear at the interface of the scalloplike IMC/(011) single crystal substrate. When a large number of IMC grains were investigated, only some special orientation relationships can be detected based on the PFs. With increasing the reflowing time, the orientation relationship has no obvious change.
(2) For Sn/(011) Cu couple, there is no obvious change for the texture intensity and the orientation relationship when the couple was aged at 50 °C for ten days. However, when the aging temperature is 170 °C, the formation of the new phase (Cu_3Sn) would destroy the orientation relationship between Cu_6Sn_5 and Cu single crystal but not decrease the texture intensity of Cu_6Sn_5 layer.
(3) Two kinds of interfacial energies were considered to explain the IMC morphology on the single crystal substrates: (1) the interfacial energy of the solder/IMC and (2) the decrease in the interfacial energy due to the orientation relationship between the IMC and substrate. The faceted-Ag_3Sn grains are always formed on the Ag single crystal with random orientation; however, the faceted Cu_6Sn_5 grains are only formed on the special Cu single crystals [e.g., (001), (111)] during the reflowing initial stage.

ACKNOWLEDGMENTS

The authors would like to thank W. Gao, H. H. Su, X. G. Liu and J. O. Suh for sample preparation, SEM observations and experimental discussion. This work was financially supported by National Basic Research Program of China under Grant No. 2010CB631006 and the National Outstanding Young Scientist Foundation under Grant No. 50625103.

[1] K. N. Tu, *Solder Joint Technology: Materials, Properties, and Reliability* (Springer, New York, 2007).
[2] T. Laurila, V. Vuorinen, and J. K. Kivilahti, Mater. Sci. Eng. R **49**, 1 (2005).
[3] M. Abtew and G. Selvaduray, Mater. Sci. Eng. R **27**, 95 (2000).
[4] K. Zeng and K. N. Tu, Mater. Sci. Eng. **38**, 55 (2002).
[5] H. K. Kim and K. N. Tu, Phys. Rev. B **53**, 16027 (1996).
[6] J. O. Suh, K. N. Tu, and N. Tamura, Appl. Phys. Lett. **91**, 051907 (2007).
[7] J. O. Suh, K. N. Tu, and N. Tamura, J. Appl. Phys. **102**, 063511 (2007).
[8] H. F. Zou, H. J. Yang, and Z. F. Zhang, Acta Mater. **56**, 2649 (2008).
[9] H. F. Zou, H. J. Yang, J. Tan, and Z. F. Zhang, J. Mater. Res. **24**, 2141 (2009).
[10] H. F. Zou, H. J. Yang, and Z. F. Zhang, J. Appl. Phys. **106**, 113512 (2009).
[11] F. J. Humphreys, J. Mater. Sci. **36**, 3833 (2001).
[12] A. Sémoroz, Y. Durandet, and M. Rappaz, Acta Mater. **49**, 529 (2001).
[13] H. J. Yang, Y. B. Xu, Y. Seki, V. F. Nesterenko, and M. A. Meyers, J. Mater. Res. **24**, 2617 (2009).
[14] A. J. Clarke, R. D. Field, R. J. McCabe, C. M. Cady, R. E. Hackenberg, and D. J. Thoma, Acta Mater. **56**, 2638 (2008).
[15] G. G. E. Seward, S. Celotto, D. J. Prior, J. Wheeler, and R. C. Pond, Acta Mater. **52**, 821 (2004).
[16] H. Sato and S. Zaefferer, Acta Mater. **57**, 1931 (2009).
[17] M. H. Lu, D. Y. Shih, P. Lauro, C. Goldsmith, and D. W. Henderson, Appl. Phys. Lett. **92**, 211909 (2008).
[18] S. Qu, X. H. An, H. J. Yang, C. X. Huang, G. Yang, Q. S. Zang, Z. G. Wang, S. D. Wu, and Z. F. Zhang, Acta Mater. **57**, 1586 (2009).
[19] W. K. Choi, S. Y. Jang, J. H. Kim, K. W. Paik, and H. M. Lee, J. Mater. Res. **17**, 597 (2002).
[20] W. E. John, *A Guide to Lead-free Solders Physical Metallurgy and Reliability* (Springer, New York, 2007).
[21] P. J. Shang, Interfacial reactions and intermetallic compiound growth between low temperature eutectic SnBi and SnIn lead-free solders and Cu substrate, PhD thesis, CAS, 2009.
[22] C. W. Fairhurst and J. B. Cohen, Acta Crystallogr., Sect. B: Struct. Crystallogr. Cryst. Chem. **28**, 371 (1972).
[23] Z. L. Li, H. B. Xu, and S. K. Gong, J. Phys. Chem. B **108**, 15165 (2004).
[24] I. Sunagawa, *Crystals: Growth, Morphology, and Perfection* (Cambridge University Press, Cambridge, 2005).
[25] J. O. Suh, K. N. Tu, G. V. Lutsenko, and A. M. Gusak, Acta Mater. **56**, 1075 (2008).